

FRACTURE OF ZIRCALOY CLADDING AS A CONSEQUENCE OF POWER INCREASES IN WATER REACTOR FUEL RODS

G. V. RANJAN

Failure Analysis Associates, 750 Welch Road, Palo Alto, California 94304, U.S.A.

E. SMITH

*Joint Manchester University/UMIST Metallurgy Department,
Grosvenor Street, Manchester M1 7HS, United Kingdom*

SUMMARY

The authors are conducting a detailed theoretical investigation, whose objective is to further our understanding of the fracture of Zircaloy cladding by interactions with Uranium Dioxide fuel pellets in water reactor fuel rods, as a consequence of a power increase after a sufficiently high burn-up. To accommodate the thermal expansion in the outer regions of the fuel pellets, radial cracks form within the fuel, and the Zircaloy cladding deforms in response to the fuel expansion, stress corrosion cracks forming and growing within the cladding in the vicinity of the fuel pellet cracks; these lead to cladding failure and iodine is generally regarded as being one of the active chemical species.

The investigation is based on the development and analytical solution of simplified models that represent the formation and growth of the Zircaloy stress corrosion cracks, but the analyses are also supported by finite element studies where appropriate. The initial results from the investigation, presented at the recent ASTM Conference on "Zirconium in Nuclear Applications", Quebec City, August 1976, showed that stress corrosion crack growth in irradiated Zircaloy must be able to proceed at very low stress intensifications if uniform friction effects are operative at the fuel-cladding interface, when the interfacial friction coefficient is less than unity, when a symmetric distribution of fuel cracks exists, and when symmetric interfacial slippage occurs (i.e. "uniform" conditions). Otherwise, the observed fuel rod failures must be due to departures from "uniform" conditions and a very high interfacial friction coefficient, and particularly fuel-cladding bonding, are means of providing sufficient stress intensification at a cladding crack tip to explain the occurrence of cladding fractures.

Since the preparation of the Quebec paper, the research has followed three main lines with the following results:

- (a) The Quebec results were based on the use of an extremely simple mode III simulation model, and the analysis has been repeated using a mode I model which is more representative of the real situation; the earlier conclusions remain essentially unchanged.
- (b) A detailed assessment of these results against the background of available experimental evidence enables us to take the viewpoint that crack nucleation is likely to be the controlling event in the failure of Zircaloy cladding during a power ramp.
- (c) Further and more detailed consideration has been given to the role of fuel-cladding interfacial frictional effects, and results from an analysis of the fuel cracking characteristics suggests that high interfacial frictional forces are unlikely to be operative during a power ramp.

Results from (c), coupled with those mentioned in (a), provide support for the viewpoint that crack nucleation in Zircaloy cladding is the critical event in the failure process. Accordingly detailed consideration is now being given to the development of an understanding of cladding crack nucleation, with the objective of formulating a failure criterion that can be linked with an integrated fuel-cladding computer code.

1. Introduction

Experience with uranium dioxide fuel, clad in Zircaloy tubing, has shown that a sudden power increase (ramp) can, after a sufficiently high burn-up, lead to cladding failure. The main problem has been with CANDU and BWR fuel rods, and although PWR failures have occurred, the problem is not as extensive, presumably because the PWR designs are such that power changes are not so abrupt. It has been demonstrated that operational and design parameters such as ramp magnitude, ramp rate and the as-assembled gap between fuel and cladding, play major roles in determining whether fuel rod failure occurs. A power increase generates a temperature gradient within the uranium dioxide fuel pellets such that the inner regions are at maximum temperature; to accommodate the thermal expansion of these regions, radial cracks form in the outer pellet regions. The Zircaloy cladding deforms in response to the fuel expansion, and the high cladding strains and increased amount of fission products in the vicinity of the fuel cracks contribute to cladding fracture by crack formation and growth.

Important features of these power ramp cladding fractures are [1]:

- * They are usually characterized by an absence of general cladding deformation.
- * Unless a power ramp is particularly severe, the fracture surface is macroscopically flat with little evidence of extended 45° shear fracture segments, except perhaps near the outer cladding surface.
- * Partial penetration cracks are sometimes observed; their openings are appreciably less than their lengths.
- * There is often a time delay of several hours between a power ramp and a fuel rod failure signal.
- * Fuel rod failure does not occur if unirradiated uranium dioxide is sheathed by irradiated Zircaloy and the rods are subjected to power ramps at negligible burn-up; this indicates that the local stressing of neutron embrittled Zircaloy, in the vicinity of pellet cracks, is insufficient in itself to rupture the cladding in the absence of fission products.
- * If the time at high power during a ramp is small, cladding fracture does not occur.
- * The surface appearance of a cladding fracture is similar to that of an iodine stress corrosion failure in a controlled laboratory experiment.

In accord with the viewpoint adopted by many workers, these observations strongly suggest that fuel rod failures, to which the characteristics given above refer, are of the stress corrosion type, and iodine is generally regarded as being one of the active chemical species.

2. Scope and Objectives of the Investigation

The present theoretical investigation concentrates on cladding fractures, associated with fuel pellet cracks and having the characteristics described in the Introduction, and proceeds from the basis that fracture occurs by a stress corrosion mechanism. The investigation develops and analyses simplified models which represent the real situation. Consequently, the approach has several attributes: for example, it enables the physics of the problem to be readily appreciated and it provides clear guidelines for complementary experiments, with which it can interact. Furthermore, recognizing that the complexity of

the behaviour of an actual power reactor fuel rod necessitates the use of a computer model to specify operational criteria, i.e. a maximum permissible ramp size and ramp rate at a given burn-up, the simplified procedures facilitate the incorporation of the appropriate physical mechanisms and failure criteria into the computer code. They can also indicate possible modifications to the metallurgical structure of the fuel and cladding, or the fuel-cladding interfacial conditions, which will reduce or eliminate the incidence of fuel rod failures.

To provide a starting point for this wide-ranging theoretical study of the cladding fracture problem, which forms part of the Electric Power Research Institute Fuel Rod Performance Program, this paper explores the growth behaviour of cladding cracks using standard linear elastic fracture mechanics procedures. This aspect of the overall problem was initially investigated using an extremely idealized model, and the results were reported [2] at the recent Quebec City Symposium on Zirconium in Nuclear Applications. Because of this idealization, the specific study described in this paper was viewed to be essential; in the event, it transpires that this new analysis, which is based on a vastly more realistic model, gives conclusions which are similar to those presented at Quebec City.

3. Analysis of Fuel-Cladding Interaction Effects

3.1 The Average Strain within the Cladding near a Fuel Pellet Crack

From the observations described in the Introduction it is clear that the stress corrosion cracks propagate without the cladding exhibiting general yield; this is evidenced by partial penetration cracks having small openings as compared to their lengths. Consequently, the deformation behaviour of the cladding may be described by elastic thin shell theory, which gives the average, with respect to the cladding thickness, hoop stress and strain within the cladding as a function of the polar angle θ measured from a fuel pellet crack. The basis for the investigation is Gittus' model [3,4] (Fig. 1) where there is a symmetric distribution of N fuel pellet cracks and symmetric interfacial slippage, with μ being the interfacial friction coefficient; the fuel pellet radius and cladding thickness are respectively R and t . Elastic thin shell analysis gives the strain ϵ as [2]

$$\epsilon = \frac{\epsilon_{\text{MEAN}} \mu \theta_{\text{MAX}} \exp(-\mu\theta)}{[1 - \exp(-\mu\theta_{\text{MAX}})]} \quad (1)$$

where ϵ_{MEAN} is the mean cladding hoop strain, as measured circumferentially, and $\theta_{\text{MAX}} = \pi/N$ is the extent over which interfacial slippage occurs in the same direction. If $\mu\pi/N = \mu\theta_{\text{MAX}}$ is small, say $\sim 1/3$ (for example, when $\mu = 1$ and $N = 10$) ϵ does not vary with θ by more than 25%, and it is then a reasonable approximation to assume that it has the uniform value ϵ_{MEAN} for all θ .

3.2 Fuel-Cladding Interfacial Stresses

As indicated previously, elastic thin shell theory upon which the preceding discussion is based, gives the average hoop stress and strain distributions. However, in the real situation, the hoop stress and strain peak at the inner cladding surface, and the effect of this high local stress must obviously be examined with regard to the growth of any cladding crack that might form near a fuel pellet crack. Therefore, it is essential to determine the actual stress distribution within the cladding near a fuel pellet crack and more particularly the hoop stress variation in the thickness direction, since this stress is

responsible for the growth of a crack that is normal to the cladding surface (Fig. 2). Although thin shell theory does not give this hoop stress variation directly, it nevertheless does give the interfacial stresses that can be used as boundary conditions for the determination of the actual stress distribution within the cladding. At a point on the interface, the normal pressure is

$$P_N = \frac{Et\epsilon}{R} \sim \frac{Et\epsilon_{MEAN}}{R} \quad (2)$$

irrespective of the angular distance θ from a pellet crack, where E is the Young's modulus of the cladding. Furthermore, the interfacial shear stress $P_S = \mu P_N$ is given by

$$P_S \sim \frac{\mu Et\epsilon_{MEAN}}{R} \quad (3)$$

These values for P_S and P_N will now be used as input information for the determination of the local stress distribution within the cladding near a fuel pellet crack.

3.3 Local Stress within the Cladding near a Fuel Pellet Crack

The uniform normal pressure P_N , see Eq. (2), at the fuel-cladding interface produces a constant hoop stress $E\epsilon_{MEAN}$ within the cladding if t is small compared with R . However, it is more difficult to assess the effect of the shear stress P_S , see Eq. (3), that causes the peaking of the cladding hoop stress at the inner cladding surface, because it changes sign at each pellet crack and at the points midway between pellet cracks. Since the effect of curvature will not be significant, one can use the plane strain (Mode I) model (Fig. 3), where $\sigma_I \equiv \mu Et\epsilon_{MEAN}/R$ and $a \equiv R\theta_{MAX}$. The objective is to determine the p_{xx} component of stress along the y axis, produced by shear stresses p_{xy} applied to the surface $y = 0$ as shown, and then associate this p_{xx} stress with the cladding hoop stress immediately ahead of a fuel pellet crack in the actual situation. In the initial analysis of this problem, which was reported at the Quebec City Conference [2], an antiplane strain (Mode III) model was used to simulate the real situation and facilitate the analysis; the Mode I analysis described in this section was conducted to see whether or not the earlier conclusions are valid, since there is clearly considerable doubt concerning the validity of a Mode III model, especially as local bending stresses are present in the Mode I model but are absent in the Mode III model.

The local stress near the origin is of the form

$$p_{xx} = \frac{4\sigma_I}{\pi} \log\left(\frac{a}{y}\right) \quad (4)$$

as is shown by taking $t = \infty$, considering the effect of equal and opposite point forces applied at $x = \pm\lambda$, $y = 0$ in the x direction, and integrating over the intervals $\lambda = -a$ to $\lambda = 0$ and $\lambda = 0$ to $\lambda = a$ to give the effect due to uniform shear stresses $p_{xy} = +\sigma_I$ applied over the interval $-a < x < 0$ and $p_{xy} = -\sigma_I$ over the interval $0 < x < a$. In accord with simple bending theory, it is then reasonable to assume that the p_{xx} stress along the y axis takes the approximate form

$$p_{xx}(x = 0) = \frac{4\sigma_I}{\pi} \log\left(\frac{a}{y}\right) + A\sigma_I + B\sigma_I y \quad (5)$$

where A and B are constants. Without going into details which are recorded elsewhere [5],

symmetry considerations and force and moment equilibrium requirements for the element bounded by $x = 0$, $x = a$ and $y = 0$, $y = t$, enable A and B to be determined, whereupon

$$\frac{P_{xx}(x=0)}{\sigma_I} = \frac{4}{\pi} \log\left(\frac{t}{y}\right) + \left(\frac{2a}{t} - \frac{10}{\pi}\right) - \frac{6y}{t} \left(\frac{a}{2t} - \frac{2}{\pi}\right) \quad (6)$$

a relation which expresses $p_{xx}(x=0)$ as a function of y , in terms of the parameters σ_I , t and a . To assess the accuracy of this approximate analytical expression for p_{xx} , finite element studies have been conducted for the specific situations where $a/t = 5$ and $a/t = 10$, and the results compared with results obtained from Eq. (6). There is excellent agreement between the two sets of results, as Figure 4 shows for the case where $a/t = 5$, and consequently Eq. (6) may be used with $a \equiv R\theta_{MAX}$ and $\sigma_I \equiv \mu E t \epsilon_{MEAN}/R$ to give the cladding hoop stress ahead of a fuel pellet crack as

$$\frac{P_{\theta\theta}(r)}{\left[\frac{\mu E t \epsilon_{MEAN}}{R}\right]} = \frac{4}{\pi} \log\left(\frac{t}{r}\right) + \left(\frac{2R\theta_{MAX}}{t} - \frac{10}{\pi}\right) - \frac{6r}{t} \left(\frac{R\theta_{MAX}}{2t} - \frac{2}{\pi}\right) \quad (7)$$

Since the specific interest concerns situations where, typically, $R/t = 10$, $N = 10$ (i.e. $\theta_{MAX} = \pi/N = 0.31$), and r/t is at most equal to 0.2, one can neglect the last term on the right-hand side of Eq. (7), which then simplifies to

$$\frac{P_{\theta\theta}(r)}{\left[\frac{\mu E t \epsilon_{MEAN}}{R}\right]} = \frac{4}{\pi} \log\left(\frac{t}{r}\right) + \left(\frac{2R\theta_{MAX}}{t} - \frac{10}{\pi}\right) \quad (8)$$

Because the interfacial normal stress produces a uniform cladding hoop stress $E \epsilon_{MEAN}$, the total hoop stress is therefore

$$P_{\theta\theta}(r) = E \epsilon_{MEAN} \left[1 + \frac{\mu t}{R} \left(\frac{2R\theta_{MAX}}{t} - \frac{10}{\pi}\right) + \frac{4\mu t}{\pi R} \log\left(\frac{t}{r}\right) \right] \quad (9)$$

This result will be used to determine the stress intensification at the tip of a cladding crack, which is normal to the inner cladding surface and contiguous with its associated fuel pellet crack (Fig. 2).

3.4 Stress Intensification at the Tip of a Cladding Crack

To simplify calculation of the stress intensification K at the tip of a crack emanating from the inner cladding surface, it is reasonable to assume that K will have the same value as that for a crack penetrating the surface of a semi-infinite solid with the crack faces being subject to the pressure distribution given by Eq. (9); this approximation is valid when the crack length c is less than $t/2$ because the effect of the outer cladding surface can then be ignored. Since the hoop stress is a monotonically decreasing function of r , the stress intensification factor at the crack tip will be approximately the same as that for the situation where the pressure distribution given by Eq. (9) is averaged-out along the crack faces, i.e.

$$K \sim \sqrt{\pi c} \left[\frac{1}{c} \int_0^c P_{\theta\theta}(r) dr \right] \quad (10)$$

whereupon Eqs. (9) and (10) give

$$K \sim E c_{MEAN} \left[1 + \frac{\mu t}{R} \left(\frac{2R\theta_{MAX}}{t} - \frac{10}{\pi} \right) + \frac{4\mu t}{R} \left(1 + \log\left(\frac{t}{c}\right) \right) \right] \sqrt{\pi c} \quad (11)$$

This expression consists of three contributions that are represented by the various terms in the square bracket:

- * A contribution due to the uniform stress arising from the interfacial normal pressure P_N ; this is the unity term.
- * A contribution that is due essentially to the average stress at the inner cladding surface arising from the interfacial shear stress P_S ; this is the second term.
- * A contribution due to the highly localized effect of the interfacial shear stress P_S ; this is the third term.

3.5 Implications of the Stress Intensification Results to the Stress Corrosion Growth of a Cladding Crack

With regard to cladding crack growth by a stress corrosion mechanism, it is necessary to consider in detail the variation of K with crack size. Thus, with values of $t = 0.03$ in., $R/t = 10$ (i.e. $\mu\pi/N$ is small) and a friction coefficient μ as high as unity, Eq. (11) shows that the stress intensification at a cladding crack tip is dominated, within the crack size range $0.01 < c/t < 0.2$ by the first term, which arises from the uniform stress produced by the interfacial normal stress P_N . At the upper limit $c/t = 0.2$, the magnitudes of the various terms in the square bracket in Eq. (11) are 1, 0.30, and 0.33, while at the lower limit of $c/t = 0.01$, the magnitudes are 1, 0.30, and 0.72. More importantly, even when the cladding is stressed to general yield, with say $E c_{MEAN} \sim 50$ Ksi, which is an appropriate value for the yield stress of irradiated Zircaloy, the stress intensification is only $3 \text{ Ksi}\cdot\sqrt{\text{in.}}$ when $c/t = 0.01$ and $11 \text{ Ksi}\cdot\sqrt{\text{in.}}$ when the crack has grown to $c/t = 0.2$. The corresponding values for the stress intensification obtained by the Quebec City paper's idealized analysis [2] are $2.5 \text{ Ksi}\cdot\sqrt{\text{in.}}$ and $10 \text{ Ksi}\cdot\sqrt{\text{in.}}$; the similarity between the two sets of values is remarkable in view of the idealization of the Quebec City paper's model.

The general conclusions are therefore similar, and accordingly, on the basis of this paper's analysis, for failure to occur within a few hours after a power ramp, crack growth at a rate of 10^{-4} to 10^{-3} ins. per min. must be able to proceed at K values not appreciably in excess of $\sim 3 \text{ Ksi}\cdot\sqrt{\text{in.}}$.

4. Discussion

The preceding section has modelled the fracture of Zircaloy fuel rod cladding by a stress corrosion mechanism for so-called 'uniform' conditions, i.e. where uniform friction effects are operative at the fuel-cladding interface, the interfacial friction coefficient is less than unity, a symmetric distribution of fuel cracks exists, and symmetric interfacial slippage occurs. The driving force for crack propagation is the stress intensification arising from the stresses caused by fuel-cladding interactions. The stress intensification is dependent upon the mean cladding hoop strain ϵ_{MEAN} which may be regarded as a quantitative measure of the ramp size, but it must be emphasized that ramp size is not the only parameter that determines whether cladding fracture occurs. Ramp rate is also very

important, since the attainment of high cladding stresses and, therefore, a high crack tip stress intensification depends on there being no significant fuel or cladding creep. A complete analysis incorporating these effects requires a coupling of the fuel and cladding mechanical behaviours, and a computerized model of the fuel rod is essential. The analytical model employed in this paper has neglected relaxation effects and, therefore, essentially provides an upper bound value for the stress intensification. In the same context, the paper has been concerned with cladding cracks which are associated with fuel cracks that are 'unopened' prior to a power ramp, because such fuel cracks provide the most severe conditions for cladding fracture.

For the 'uniform' conditions investigated, it has been assumed that $\mu\pi/N$ is small (say $< 1/3$), whereupon the approach may be viewed as a 'weak interaction theory'. On the basis of the present paper's analysis, it has been shown that K_{ISCC} for irradiated Zircaloy must be low ($\approx 3 \text{ Ksi}\cdot\sqrt{\text{in.}}$) to explain the occurrence of cladding fractures. This is a very low value for K_{ISCC} , the limiting stress intensification below which there is no measurable crack growth, although the stress corrosion cracking resistance of irradiated Zircaloy could be low because of dislocation channeling and flow concentration effects [6-9]. The analysis, therefore, focusses attention on the necessity for reliable experimental data on the variation of crack growth rate with stress intensification for irradiated Zircaloy in the presence of appropriate corrosive environments. If K_{ISCC} for irradiated material is as high as say $10 \text{ Ksi}\cdot\sqrt{\text{in.}}$, it would be difficult to explain, on the basis of this paper's analysis, the occurrence of stress corrosion cladding fractures if only 'uniform' conditions, as defined in this paper, are operative. It is, therefore, logical that the consequences of departures from these conditions should be examined. Clearly a small value of N , the number of fuel pellet cracks, and a large interfacial friction coefficient μ will give crack tip stress intensifications greater than those obtained in this paper. With regard to the former, it should be emphasized that N is the number of 'effective' pellet cracks. The fuel expansion may be sufficiently irregular that fuel-cladding slippage proceeds in the same direction for a number of adjacent pellet segments, and although the actual number of fuel pellet cracks might be large, the number of pellet crack tips, at which cladding strains are concentrated, could be small, indeed as low as unity. If this is the case, the low incidence of cladding cracks in relation to fuel pellet cracks is readily explained.

However, a more effective way of attaining a large stress intensification is to have a large coefficient of friction at the fuel-cladding interface. This coefficient may be uniformly large over the complete interface or, more likely, it may have larger values in particular regions, such as a pellet-pellet interface where there is a ridge in the cladding [10], or where there is bonding between fuel and cladding over finite interfacial intervals. In this context the observations [11] of cladding cracks in the vicinity of fuel-cladding bonding in certain Maine Yankee Core I fuel rods are of considerable interest. The association of cladding cracks with very high friction regions is certainly an attractive explanation for the limited number of cladding cracks that are observed.

These various possible alternatives, and indeed the validity of applying linear elastic fracture mechanics principles to small cracks subject to relatively high crack tip stress intensifications, are being explored in detail. The findings will be reported at

the American Nuclear Society Topical Meeting (St. Charles, Illinois) on Water Reactor Fuel Performance in May 1977, the main objective of this paper having been to present the necessary basis for these explorations; this basis has been obtained by building on the preliminary and tentative analysis presented at Quebec City.

5. Conclusions

The results presented in this paper secure the tentative position outlined in an earlier paper [2], and provide a firm basis for a detailed exploration of stress corrosion fracture of Zircaloy cladding, due to the power ramping of a water-cooled reactor fuel rod. The main conclusions are:

- (i) If experiments reveal that K_{ISCC} for irradiated Zircaloy is very low, i.e. of the order of $1 \text{ Ksi} \cdot \sqrt{\text{in.}}$, fuel rod cladding failures can be explained by the theory presented in this paper, which is appropriate for 'uniform' interfacial conditions and for small $\mu\pi/N$; growth of cladding cracks near fuel pellet chips would be possible in such conditions. Since this implies an easy crack propagation mechanism, the limited number of cladding cracks actually observed would be explained in terms of a difficulty in crack nucleation, which is then the critical event in the failure process.
- (ii) However, in the event of K_{ISCC} for irradiated Zircaloy being relatively large, the present analysis shows that cladding fractures could be due to departures from 'uniform' and small $\mu\pi/N$ conditions. A high interfacial friction coefficient and, in the extreme case, fuel-cladding bonding, are likely causes of such departures.
- (iii) A major consequence of the present analysis is the focussing of attention on two specific points: the necessity for reliable experimental data on the stress corrosion crack growth behaviour of irradiated Zircaloy, and the necessity for further field observations on the correlation between cladding fracture and localized fuel-cladding bonding.

6. Acknowledgments

This work has been performed as part of the Electric Power Research Institute Light Water Reactor Fuel Rod Performance Program (EPRI Special Report SR 25, December 1975) under contract RP 217-1 to Failure Analysis Associates. The authors are indebted to several colleagues, particularly to Dr. F. Gelhaus, Dr. C.A. Rau, Jr., and Dr. J.T.A. Roberts for valuable discussions throughout the work; they also thank Mr. R.C. Cipolla for his guidance with regard to the numerical studies.

REFERENCES

- [1] COX, B., WOOD, J.C., Electrochemical Society Symposium on Corrosion Problems in Energy Conversion and Generation, New York City, 1974, p. 275.
- [2] SMITH, E., ASTM Symposium on Zirconium in Nuclear Applications, Quebec City, Canada, August 1976 (Proceedings to be published).
- [3] GITTUS, J.H., HOWL, D.A., HUGHES, H., Nuclear Applications and Technology, Vol. 9, 1970, p. 40.
- [4] GITTUS, J.H., Nuclear Engineering and Design, Vol. 18, 1972, p. 69.
- [5] SMITH, E., RANJAN, G.V., CIPOLLA, R.C., EPRI Topical Report.
- [6] COLEMAN, C.E., MILLS, D., VAN DER KUR, J., Canadian Metallurgical Quarterly, Vol. 11, 1972, p. 91.
- [7] BELL, W.L., Zirconium in Nuclear Applications, ASTM-STP-551, 1974, p. 199.
- [8] RIEGER, G.F., LEE, D., Zirconium in Nuclear Applications, ASTM-STP-551, 1974, p. 355.
- [9] ROSENBAUM, H.S., RIEGER, G.F., LEE, D., Metallurgical Transactions, Vol. 5, 1974, p. 1867.
- [10] AAS, S., Nuclear Engineering and Design, Vol. 21, 1972, p. 237.
- [11] Joint CE/EPRI Fuel Performance Evaluation Program, Task C - Evaluation of Fuel Rod Performance in Main Yankee Core I, Final Report, July 1976 (to be published).

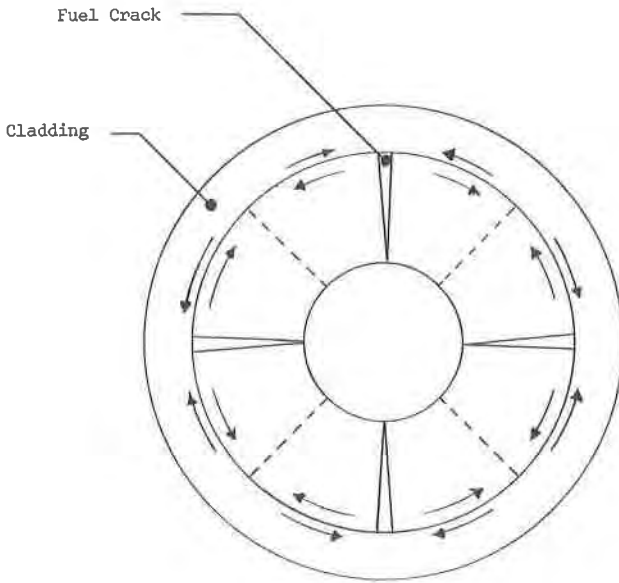


Figure 1 : The Basic Thin Shell Model Representing Pellet-Clad Interaction (PCI); The Associated Theory Gives the Average (With Respect to Thickness) Hoop Cladding Stress and Strain.

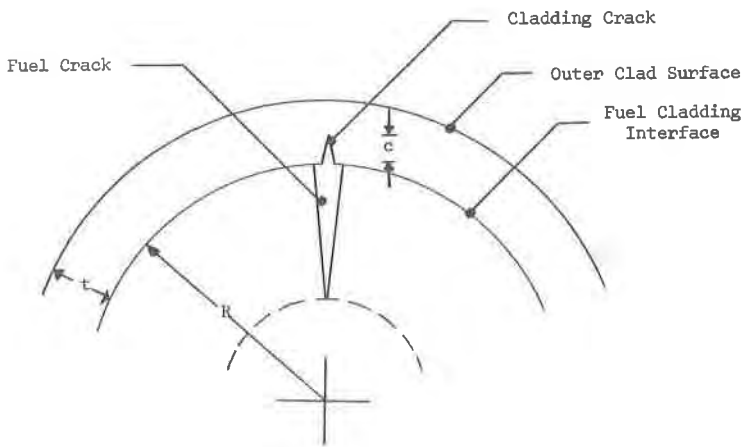


Figure 2 : Growth of a Cladding Crack Associated With a Fuel Pellet Crack.

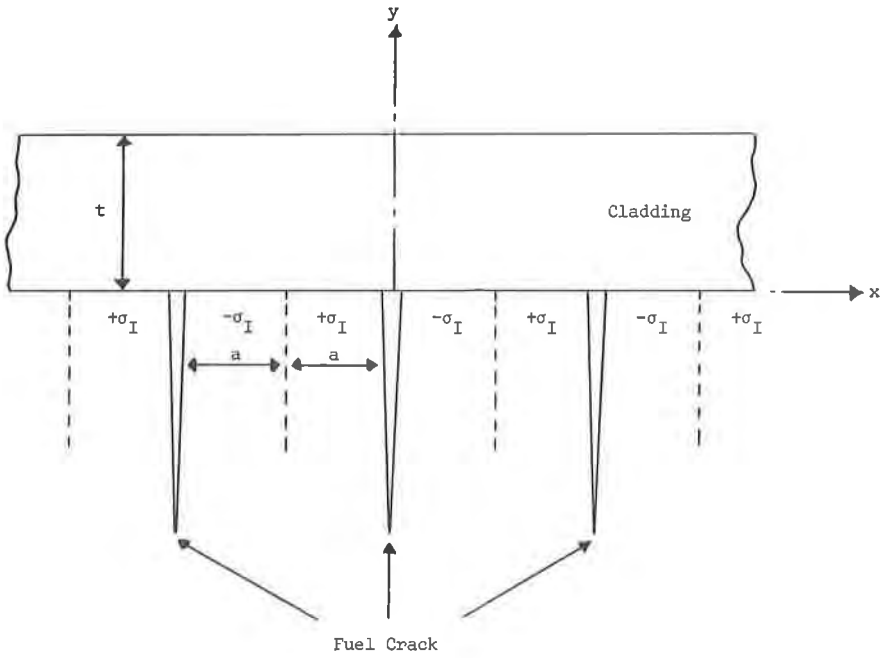


Figure 3 : The Plane Strain (Mode I) Simulation Model Used to Estimate the Effect of the Interfacial Shear Stress on the Cladding Stress Distribution.

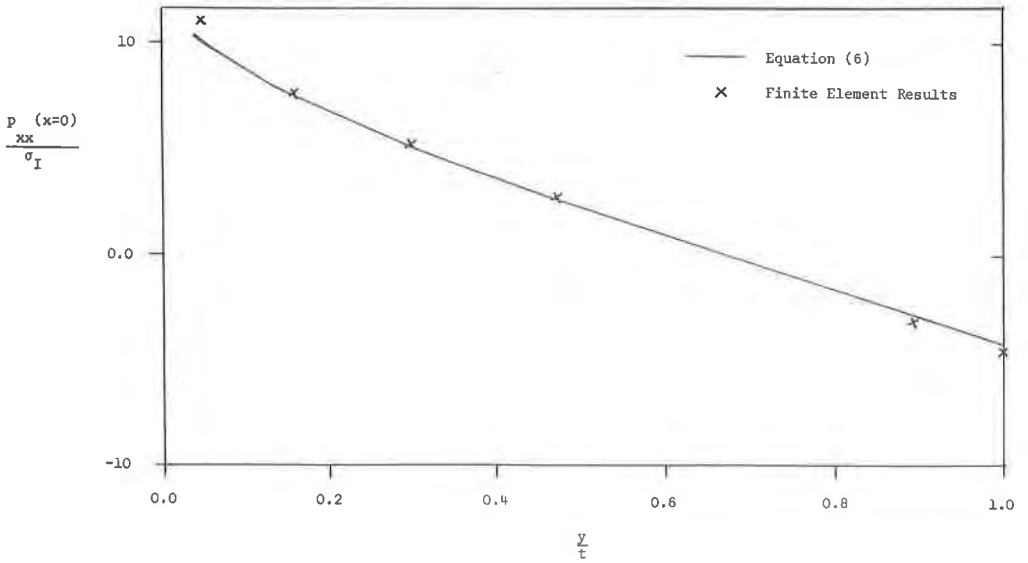


Figure 4 : Comparison of Analytical and Numerical Results with $a/t = 5$.